Journal of Coastal Research	25	3	641–650	West Palm Beach, Florida	May 2009

Sedimentary and Geochemical Signatures of Depositional Environment of Sediments in Mudflats from a Microtidal Kalinadi Estuary, Central West Coast of India

Ksh. Tomchou Singh and G.N. Nayak

Department of Marine Sciences
Goa University
Goa, India 403 206
gnnayak@unigoa.ac.in

ABSTRACT

SINGH, KSH. TOMCHOU and NAYAK, G.N., 2009. Sedimentary and geochemical signatures of depositional environment of sediments in mudflats from a microtidal Kalinadi estuary, central west coast of India. *Journal of Coastal Research,* 25(3), 641–650. West Palm Beach (Florida), ISSN 0749-0208.

A detailed study of sediment components and selected metals has been carried out in two mudflat cores collected from the creeks of Kalinadi Estuary, India, in order to assess the variations in distribution of sediment components, metals, and the controlling processes, including early diagenetic movements, if any. Grain size analyses reveal the possibilities of three episodes of deposition in a highly varying depositional environment with overall fining up of the cores. Organic carbon (OC) is comparatively high in muddy Core KM, which was collected from a more sheltered creek with a narrow mouth in the estuarine interior, than sandy Core KH, which was collected from a creek with a wide mouth nearer to the sea. Geochemical data show an upper zone of marked enrichment of all trace metals, including Fe and Mn, in both the cores. The variations in sediment components as well as associated metals between the two cores reveal variations in controlling factors including the morphology setup. The distribution of trace metals in Core KH are controlled by the proportions of finer fraction of sediments, degradation of organic carbon, and redox-sensitive Fe and Mn oxides, while the distribution of trace metals in Core KM are probably controlled by the finer sediments as well as by redox-sensitive Fe and Mn oxides.

ADDITIONAL INDEX WORDS: *Mudflats, sedimentary, early diagenesis, geochemistry, cores, Kalinadi Estuary.*

INTRODUCTION

Intertidal mudflats are a prominent geomorphological component of estuaries, and the development of an estuarine mudflat is both complex and difficult to predict because of the multiple relationships between the physical, chemical, and biological properties of the sediment (Patersion, Crawford, and Little, 1990; Yallop *et al.,* 1994). Mudflats present in the middle and lower portion of estuaries mainly consist of clay and silt, which are generally from two different sources (Lesueur *et al.,* 2003): terrigenous materials and marine particles. Despite strong hydrodynamics, estuarine mudflats are preferential sites for accumulation and preservation of sediments and organic matter, especially from numerous marine, atmospheric, and terrestrial sources including those of anthropogenic origin. Organic matter and most of the contaminants are associated with fine-grained particles, which can be trapped on mudflats (Billon, Ouddane, and Boughriet, 2002). Metal behaviour in these systems of fluvial marine interaction has aroused a growing interest among the scientific community (Borrego, Lopez-Gonzalez, and Carro, 2004). Sedimentary sequences in mudflats and tidal marshes have been extensively studied because of their demonstrated ability to preserve an undisturbed record of environmental change. A low rate of bioturbation coupled with a fairly high sedimentation rate provides an ideal substrate for the preservation and reconstruction of long-term and short-term changes in the coastal environment. Sedimentary records were used to determine the forcing processes and parameters controlling the evolution of the tidal flat on varying time scales (Allen and Duffy, 1998; O'Brien, Whitehouse, and Cramp, 2000). Within the intertidal region of an estuary, sediments are composed of different sedimentological and geochemical phases that act as potential binding sites for metals entering an estuarine system. These phases include clay, silt, sand, organic material, oxides of iron, manganese, aluminum and silica, carbonate, and sulphide complexes (Shea, 1988). Of these components, oxides of iron and manganese and organic matter are considered the most important in influencing processes of metal transport, distribution, and bioavailability (Davies-Colley, Nelson, and Williamson, 1984; Louma and Bryan, 1982; Rule and Alden, 1996). But the importance of processes contributing to the sediment matrix within a mudflat is poorly known. Hence, it is necessary to determine relative importance of diagenetic processes and riverine input in contributing to the heterogeneity in sediment distribution as well as geochemistry in these intertidal areas. However, in general, this very complex and dynamic depositional environment is inadequately documented. Further, much less research has been undertaken on estuarine mudflats as far

DOI: 10.2112/07-0954.1 received 20 October 2007; accepted in revision 24 April 2008.

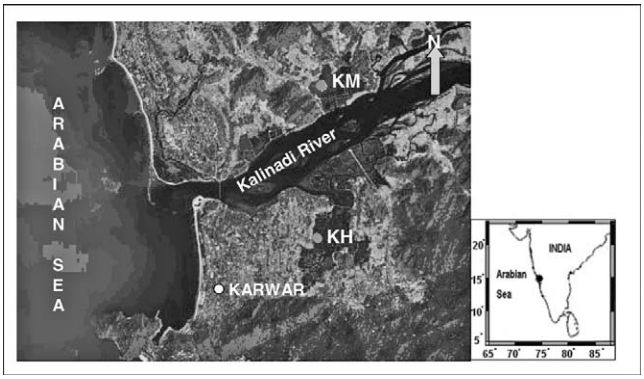

Figure 1. Study area with core locations.

as India is concerned. The present study of sedimentology and geochemistry of estuarine mudflats will provide new insights into the distribution, associated depositional environment, and postdepositional behaviour of metals with time.

STUDY AREA

Kalinadi Estuary can be classified as the drowned estuary type and is a partially mixed estuary draining into the Karwar Bay (lat 14°50′ N and long 74°07′ E) on the west coast of India (Figure 1). The tides here are semidiurnal in nature with amplitude of about 2 m. The time and range between the two floods and two ebbs show marked variations. Kalinadi is one of the rivers that traverse the Western Ghats for 184 km and join the Arabian Sea near Karwar. It has major tributaries like Pandary, Tattihalla, Kaneri, Kali, and Vaki. Narrow and small mudflats in the creeks in the lower part of the estuary characterise the Kalinadi Estuary. Although narrow and sheltered, these mudflats play an important role in trapping sediments and metals within the estuary. The Kalinadi River has a total catchment area of about 4841 km^2. The annual rainfall in this area averages about 350 cm, about 75% of which is received during the southwest monsoon (June to September). As a consequence, during this wet season considerable freshwater discharges into the Arabian Sea through the Kalinadi. Associated with this heavy rainfall, detritus from the mountain tops, hill slopes, and lowland plains are collected and transported to the sea (Nayak, 1993). Geologically, the area comprises gneiss and granite, with Dharwarian rocks like schist, amphibolite, and older metamorphic rocks within them. The other rock types present in the area are orthoquarzite, manganiferous chert and argillite, banded magnetite/hematite quartzite, limestone and dolomites, graywacke, and basic dykes. Veer, Shanmukhappa, and Bhat (1992) reported the mean concentrations of Cu, Cr, and Mn in this estuarine water as 0.11, 0.044, and 0.37 parts per million (ppm), respectively. The corresponding values for sediment are 7.022, 14.18, and 18.56 ppm on a dry weight basis. This study has also revealed that the trace metal concentration of the sediments shows an increasing trend from the mouth to the upstream. The mean grain size exhibits a marked decreasing trend on either side of the mouth of the Kali River. These variations in size parameters are attributed to the drifting of sediments on either side of the river, possibly due to cellular flows, which develop in the river mouth region (Nayak, 1996). However, as far as mudflats are concerned, no data is available; it is known that they play a significant role in trapping sediments and metals. The mudflats are flanked by mangrove vegetation, which is generally made up of the fringing type.

METHODOLOGY

Two sediment cores were collected using a hand-driven PVC coring tube. Before subsampling, each core was described with reference to color and other physical characteristics. Cores were then subsampled at 2-cm intervals with a plastic spatula to avoid metal contamination; samples were then transferred to cleaned polyethylene bags and stored in an icebox until they reached the laboratory. In the laboratory, sediments were dried at 60°C overnight and kept ready for analysis. Grain size analysis was carried out by the pipette method of Folk (1968). Organic carbon estimation was carried out by the wet oxidation methods of Gaudette *et al.* (1974), in which exothermic heating and oxidation with $K_2Cr_2O_7$ and concentrated H_2SO_4 are followed by titration of excess dichromate with 0.5 N $Fe(NH_4)_2(SO_4)_2 \cdot 6H_2O$. X-ray diffraction studies were carried out from 3 to 30° 2Θ at 1.2° 2Θ/min on a Philips X-ray diffractometer (PW 1840 model). Relative percentages of different clay minerals like kaolinite, chlotite, illite, and smectite were estimated by weighing the integrated peak areas of basal reflections in the glycolated X-ray diffractograms, following the semiquantitative method of Biscaye (1965). Sediment samples for major and trace metal analysis were digested by using hydrofluoric-perchloric-nitric acid mixtures in Teflon beakers. Complete digestion was ensured by repeating the digestion steps until clear solutions were obtained. The resultant solutions were analysed for Al, K, Mg, Ca, Fe, Mn, Zn, Cu, Cr, and Co using an atomic absorption spectrophotometer (GBC 932 AA). Precision was monitored by analysing triplicate samples for some selected samples and was generally <6 percent standard deviation (%SD) for major and trace elements. Accuracy of the method was determined by comparing with reported values of a certified standard (GSJ-JSd-1); for the working values quoted, accuracy was $\pm 3\%$ for Zn; $\pm 6\%$ for Fe and Mg; $\pm 10\%$ for Mn, Al, Ca, and K; $\pm 15\%$ for Cu; and $\pm 30\%$ for Cr and Co.

RESULTS AND DISCUSSION

Field Observations

On the field, the sediment cores could be separated into three vertical zones based on difference in sediment colour as follows:

(1) A brown top layer of sediment, 17 cm in Core KH and 18 cm in Core KM.
(2) A grey middle layer located between 17–50 cm in Core KH and 18–48 cm in Core KM.
(3) A mixed bottom layer between 50–76 cm in Core KH and 48–70 cm in Core KM.

A distinct geochemical redox profile, which is visually evi-

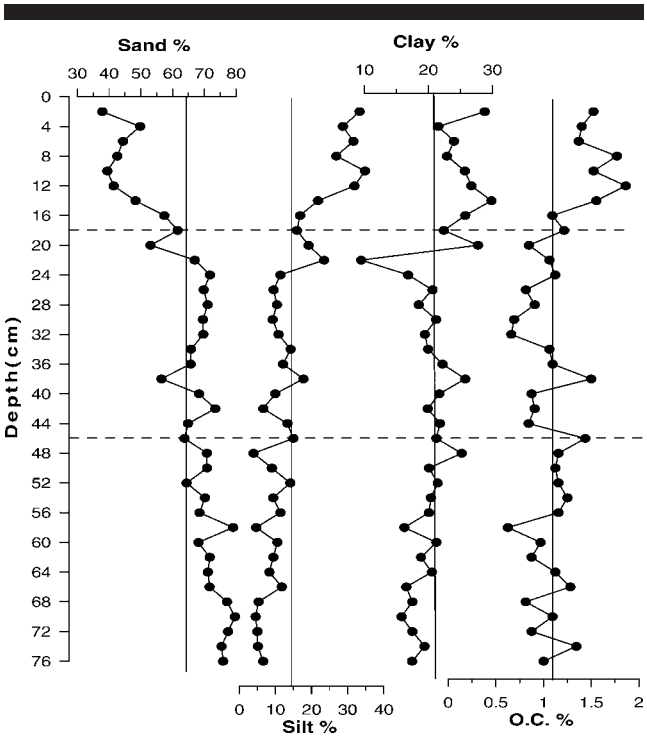

Figure 2. Downcore variations of sediment components with vertical lines of average values in Core KH.

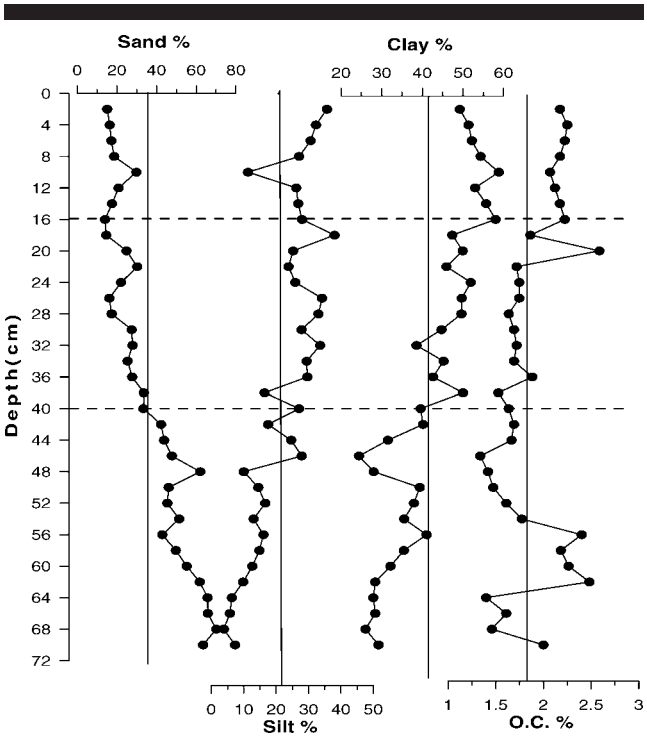

Figure 3. Downcore variations of sediment components with vertical lines of average values in Core KM.

dent, often develops in mudflats and salt marshes (Cundy and Croudace, 1995; Williams, Bubb, and Lester, 1994; Zwolsman, Berger, and Van Eck, 1993). The visual evidence is mainly due to the postdepositional relocation of the major elements Mn and Fe in the marsh profile, with formation of red/brown Mn(IV) and Fe(III) oxyhydroxides in an upper oxidized zone and of reduced black/grey Fe(II) sulfides in a deeper reducing zone (Thomson, Dyer, and Croudace, 2002). These field observations are in agreement with the downcore distribution profiles of analysed grain size components and redox-sensitive elements (Fe and Mn), which are discussed below in detail. The upper layer of the sediment shows high content of Fe and Mn, suggesting an oxic layer; concentrations decline in next two layers, supporting a reduced layer. Thus the three layers can be identified as an oxic top layer rich in clay, a reduced clayey layer, and a reduced bottom sandy layer.

Sediment Components

Grain Size

The percentage of sand, silt, and clay for each core are presented graphically (Figures 2 and 3) and described below. The data obtained shows a range of 38%–80% sand, 4%–35% silt, and 10%–30% clay for Core KH, and a range of 14%–70% sand, 4%–38% silt, and 24%–59% clay for Core KM. It is observed that in both the cores, sediment size decreases upward. However, a difference is seen in that Core KH, which was collected from a creek with a wide mouth nearer to the sea, is typically sandy, with an average of 64% sand, while Core KM, which was collected from a more sheltered creek with a much narrower mouth to the estuarine environment, is muddy, with an average of 64% mud (<63 μm) and 36% sand. In both the cores, the clay fraction is nearly constant, and the variations can be directly related to the increase in the sand fraction replacing silt with depth.

From the grain size profile with depth (Figure 2), Core KH can be divided into three sections, namely 76–46 cm, 46–18 cm, and 18–0 cm. The bottom section, 76–46 cm, is marked by the gradual decrease of sand, which is compensated by the gradual increase in both silt and clay. In the middle layer, 46–18 cm, distributions of sand, silt, and clay are near constant with some variations at a few points. In the top layer, 18–0 cm, there is a decrease in sand accompanied by an increase in silt, but the clay content varies in both directions. When the lines of average individual values of the different components are plotted with the distribution profiles of respective components, they also support the division into three core portions described above. In the bottom section, the sand is positively deviated from the average value, which is compensated by a negative deviation of silt and clay. In the middle section, all three components are consistently near their average values, while in the top layer, the sand value is less than the average calculated while the silt and clay values are more than their respective average values.

Similarly, in Core KM (Figure 3), the whole core can be divided into three different portions, but at different depths depending on the sediment components. The bottom portion,

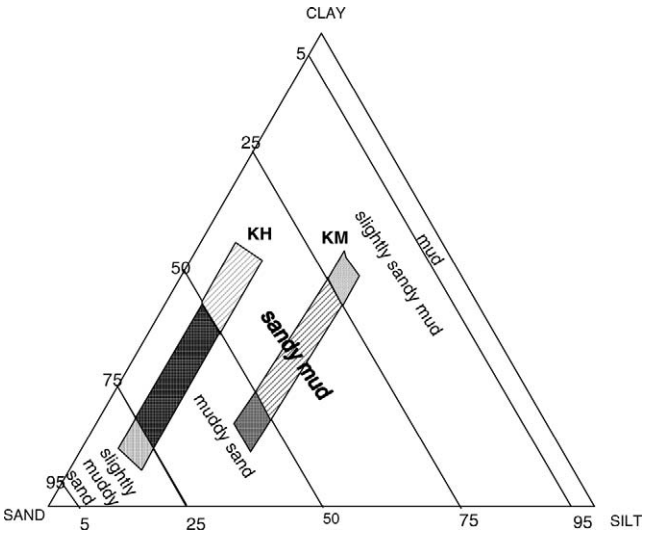

Figure 4. Ternary diagrams for a revised textural classification of sediments on the basis of sand/mud ratios after Flemming (2000).

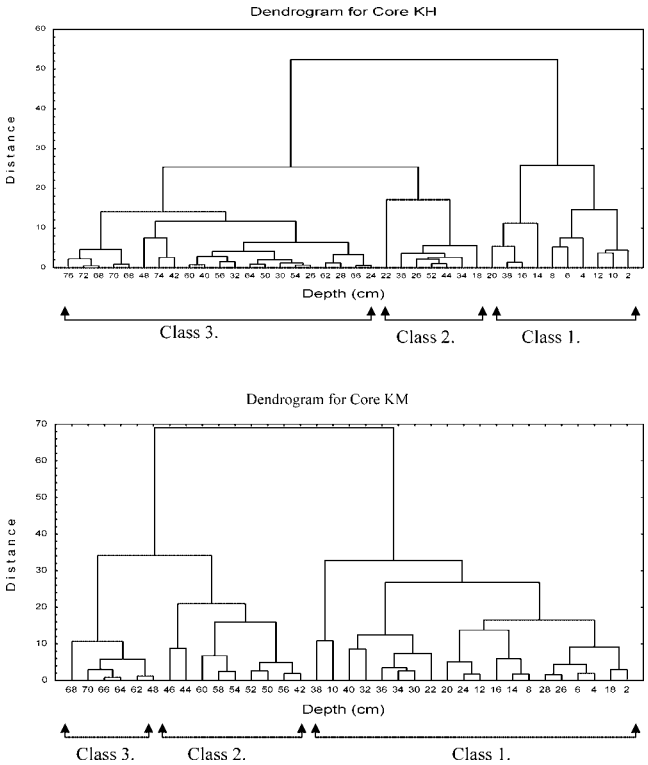

Figure 5. Dendrograms based on the complete linkage method for Core KH and Core KM.

70–40 cm, is marked by the gradual decrease in sand content, which is compensated by the gradual increase in both silt and clay. The same trend is seen in the middle portion, 40–16 cm. A nearly constant sand distribution and an increasing and decreasing profile of silt and clay, respectively, characterise the upper portion, 16–0 cm, with a break at 10 cm. The classification of the core into three portions is also supported when the depth profile is plotted with the lines of individual average values of the different components. In the bottom section, the major portion of sand profile is positively deviated while silt and clay profiles are negatively deviated from their respective lines of average value. A negatively deviated upward-decreasing profile of sand and positively deviated increasing profiles of silt and clay characterise the middle portion. The top portion is characterised by a nearly constant negatively deviated sand profile but positively deviated increasing silt and decreasing clay profile upward from their respective average value line.

Further, sediment classification has been attempted by plotting the percentage of sand, silt, and clay in a triangular diagram proposed by Flemming (2000), in order to understand the change in sediment character throughout the core and hence the depositional environment (Figure 4). It is found that both cores can be divided into three zones as follows:

Core KH		Core KM	
Depth (cm)	Lithology	Depth (cm)	Lithology
0–14	Sandy mud	0–28	Slightly sandy mud
14–66	Muddy sand	28–58	Sandy mud
66–76	Slightly muddy sand	58–70	Muddy sand

In the same way, the changes in sediment character is supported by cluster analysis in which sand, silt, clay, and organic carbon have been used. Each core can be grouped into three classes based on cluster analysis, which produced dendrograms (Figure 5). There are repetitions of groups within Core KH. The statistical data for these classes are presented in Table 1.

It can be argued that the composition of sediment simply reflects source-related features. While this holds true for the mineralogical and textural composition of many sediments, it is equally true that the source-controlled grain size spectra would still be subjected to size sorting in the course of hydrodynamic transport, which would hence result in selective deposition along an energy gradient (Bangnold, 1968). The affinity of plots to specific hydrodynamic conditions can, in fact, be demonstrated by splitting up individual data sets into discrete clusters and identifying the associated samples in an area (Flemming, 2000). In the present study, the textural gradient shows a marked change with space and time, which indicates the change in energy gradient and hence the depositional environment. In the cores studied, there are three distinct successive clusters that are very well supported by the distribution profiles of different sediment components, which probably suggests three episodes of deposition in three different environmental settings. From the textural analysis explained above as well as from grain size profiles, an upward fining trend is witnessed, *i.e.,* finer sediments are deposited more recently. All this evidence is enough to infer that the depositional environment is changing with time.

Table 1. *The mean and standard deviation (SD) of sedimentary variables defining different classes in both cores. (OC = organic carbon)*

Class	% Sand	% Silt	% Clay	% OC	
Core KH					
1.	47.01	26.28	25.55	1.44	mean
	7.01	6.84	2.58	0.30	SD
2.	64.75	15.46	19.79	1.12	mean
	1.73	3.74	4.61	0.18	SD
3.	72.46	8.24	19.29	0.99	mean
	3.57	2.61	4.61	0.21	SD
Core KM					
1.	22.52	28.10	49.38	1.94	mean
	6.54	6.20	5.49	0.29	SD
2.	47.19	17.54	35.28	1.82	mean
	4.28	5.35	5.29	0.37	SD
3.	64.84	7.12	27.99	1.82	mean
	3.14	2.40	1.07	0.42	SD

Gallagher, Wheeler, and Oxford (1996) have successfully classified the sediment core into different groups by cluster analysis and assigned different depositional facies, which were deposited in different depositional environments in two tidal marshes on the northwest coast of Ireland. Similarly Vilas *et al.* (1999) were able to show that each successive cluster within their data band corresponded to a particular depositional zone along a shore normal transect of the subantarctic macrotidal flats of San Sebastian Bay, Argentina. In addition, in this study, marked variation in sediment components between the two cores are observed that could be because of differences in geomorphology and its enhanced processes. The creek where Core KH was colleted has a wide mouth nearer to the sea through which both the tidal and river action would be relatively pronounced, resulting in the deposition of coarser fractions. On the other hand, the creek where Core KM was collected has a very narrow mouth interior to the estuarine environment through which the actions of both tides and river would be more restricted, resulting in the deposition of finer fractions.

Clay Minerals

The X-ray diffractogram (XRD) analysis was carried out for Core KH, and the identified clay minerals are kaolinite, illite, smectite, and chlorite in order of decreasing abundance (Table 2). The clay mineralogy is similar throughout the core with no major changes in the proportions of clay mineral components, which suggests little change in source or provenance over the observed sedimentation period. The composition of clay minerals, which are the weathering products of rocks and soil on land, largely depends on climate, geology, and topography of the region (Chamley, 1989; Singer, 1984). Intense chemical weathering and leaching of crystalline rocks under the tropical humid climate leads to the formation of mainly kaolinite and gibbsite (Chamley, 1989). A gneissic province is characterised by kaolinite and gibbsite that are the weathering products of Precambrian gneissic rocks and laterites of Southern India (Rao and Rao, 1995). In the present study, higher amount of kaolinite and illite clearly reflect their derivation from the catchment area, which consists mainly of Precambrian crystalline rocks that are lateritised at places. Chlorite content remained low throughout the core, which can be attributed to the prevailing humid, tropical climatic conditions in this region, wherein chlorite mineral is unstable.

Table 2. *Clay mineralogy of the selected samples in Core KH.*

Depth (cm)	% Smectite	% Illite	% Chlorite	% Kaolinite
2	11.11	29.21	8.25	51.43
18	12.42	24.42	5.47	57.63
46	9.00	26.30	2.42	62.28
72	7.72	28.39	4.59	59.29

Organic Carbon

The organic carbon (OC) content of Core KH (Figure 2) varies from a minimum of 0.63% at 58 cm, where silt and clay content is also low, to a maximum of 1.86% at 12 cm. There are three maxima of OC at depths of 38 cm, 48 cm, and 66 cm that coincide with silt and clay maxima. Organic carbon values increase from the base of the core to the surface as a whole, but it is more pronounced in the top 32 cm, where it maintains a nearly constant profile with some fluctuations downward. The decrease in OC with depth can be accounted for by the decrease of silt, to which it shows a good correlation ($R = 0.69$) compared to clay ($R = 0.48$; see Table 3). So, individually the distribution of OC with depth is more controlled by silt than clay but more significantly by mud fraction ($R = 0.70$). In Core KM, the OC value (Figure 3) shows a maximum of 2.59% at 20 cm and a minimum of 1.34% at 64 cm. As a whole, the organic carbon content increases from the base of the core, with an exception of 62–54 cm, where values suddenly rise before falling at 54 cm. Interestingly OC did not show any good correlation with either silt or clay.

The decline in OC with depth is generally attributed to degradation, and such profiles are frequently observed in sandy marine sediments. Although some degradation of organic matter must be occurring in the sediments, the dominant control on organic matter content in Core KH seems to be the proportion of mud-sized particles. The strong correlation between OC and finer fraction can be related to the pro-

Table 3. *Correlation coefficients between different parameters.*

	Fe	Mn	Zn	Cu	Cr	Co	Ca	K	Mg	Al	Sand	Silt	Clay	OC	Mud
							Core KH								
Fe	1.00														
Mn	0.87	1.00													
Zn	0.31	0.20	1.00												
Cu	0.67	0.71	0.34	1.00											
Cr	0.65	0.72	0.35	0.53	1.00										
Co	0.29	0.33	0.03	0.36	0.04	1.00									
Ca	0.08	0.05	0.36	0.17	−0.12	0.17	1.00								
K	0.65	0.62	0.16	0.46	0.56	0.22	−0.21	1.00							
Mg	0.65	0.78	0.31	0.67	0.50	0.34	0.26	0.53	1.00						
Al	0.78	0.86	0.25	0.65	0.63	0.20	0.01	0.75	0.63	1.00					
Sand	−0.89	−0.92	−0.25	−0.69	−0.74	−0.33	0.03	−0.66	−0.74	−0.79	1.00				
Silt	0.86	0.90	0.24	0.60	0.76	0.29	0.00	0.67	0.69	0.79	−0.95	1.00			
Clay	0.59	0.60	0.19	0.55	0.46	0.21	−0.04	0.44	0.56	0.49	−0.73	0.51	1.00		
OC	0.61	0.72	0.23	0.62	0.73	0.20	−0.16	0.52	0.57	0.55	−0.72	0.69	0.48	1.00	
Mud	0.88	0.90	0.25	0.66	0.74	0.30	−0.02	0.67	0.73	0.79	−0.99	0.95	0.75	0.70	1.00
							Core KM								
Fe	1.00														
Mn	0.87	1.00													
Zn	0.55	0.46	1.00												
Cu	0.80	0.59	0.71	1.00											
Cr	0.57	0.46	0.15	0.52	1.00										
Co	0.71	0.79	0.66	0.55	0.27	1.00									
Ca	0.13	0.15	0.27	0.21	−0.07	0.05	1.00								
K	0.89	0.85	0.67	0.74	0.45	0.77	0.11	1.00							
Mg	0.59	0.59	0.41	0.55	0.45	0.45	−0.23	0.67	1.00						
Al	0.90	0.81	0.66	0.75	0.32	0.76	0.32	0.87	0.48	1.00					
Sand	−0.88	−0.90	−0.67	−0.71	−0.42	−0.80	−0.17	−0.89	−0.68	−0.85	1.00				
Silt	0.78	0.77	0.68	0.67	0.47	0.70	0.39	0.76	0.51	0.78	−0.89	1.00			
Clay	0.79	0.83	0.52	0.60	0.28	0.74	−0.08	0.84	0.70	0.75	−0.90	0.61	1.00		
OC	0.23	0.36	0.03	0.01	−0.09	0.21	−0.29	0.34	0.36	0.16	−0.33	0.16	0.42	1.00	
Mud	0.88	0.90	0.67	0.71	0.42	0.80	0.17	0.89	0.68	0.85	−1.00	0.89	0.90	0.33	1.00

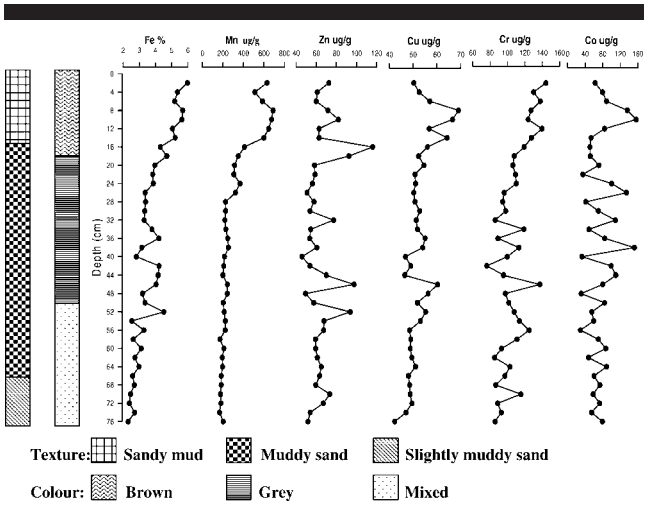

Figure 6. Downcore variations of metals in Core KH.

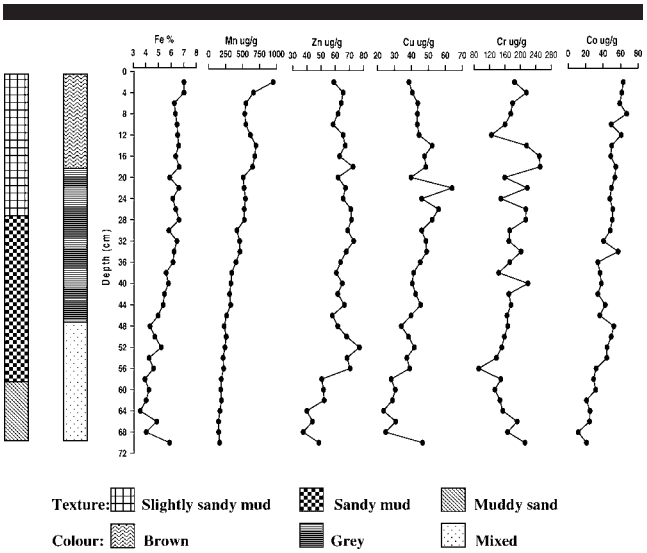

Figure 7. Downcore variations of metals in Core KM.

cess of organic matter preservation by sorption onto finer particles. However, in Core KM, the profile is different, showing relatively poor correlation with mud. This signifies that in a low-energy environment, organic carbon is not necessarily associated with fine sediments.

Metal Geochemistry

Vertical Variations

Data for selected metals analysed (Fe, Mn, Zn, Cu, Cr, and Co) for the two cores are presented graphically in Figures 6 and 7. Heavy metals have been observed to be mainly associated with fine sediments (especially clay), associated Fe/Mn, and organic coatings which provide reactive sites for metal sorption (Grant and Middleton, 1990; Cundy and Croudace, 1995). At the same time, the diagenetic cycles of Fe and Mn are well known. Therefore, the presence of a strong Fe and Mn peak may indicate redox mobilization and trace metals originally associated with the Fe/Mn substrate (McCaffrey and Thomson, 1980; Zwolsman, Berger, and Van Eck, 1993). Recognizing that the elements exhibiting the largest signals are Fe/Mn, the redox status of the cores will be inferred mainly from these elements together with the changes in colour observed in the field.

Fe and Mn

Iron and Manganese distribution profiles are quite similar in both the cores, reflecting the similar source and/or postdepositional behaviours. The concentration of Fe in Core KH increases gradually from the bottom to 54 cm; from this depth it shows some apparent peaks up to 32 cm and then increases towards the surface of the core. In Core KM, the Fe value decreases from the base of the core to 64 cm, from where it gradually increases toward the surface of the core. However, Mn concentrations show enrichment in the upper 16 cm of Core KH and 20 cm of Core KM; below this, the values decline steadily to the bottom of each core. These features are probably caused by the dissolution of Fe and Mn oxyhydroxides in the partly reduced sediment layer, by upward migration, and by reprecipitation near the oxic-suboxic interface. Diagenetic Fe enrichment starts at a greater depth than diagenetic Mn enrichment because of the somewhat higher stability of Fe oxyhydroxides under mildly reducing conditions and the faster oxidation kinetics (Selvaraj *et al.,* 2003; Zwolsman, Berger, and Van Eck, 1993). The Mn maximum in the top 16 cm in Core KH and 20 cm in Core KM probably indicates an oxic-suboxic zonation, which is also supported by the brown colour described above (Figures 6 and 7).

Trace Metals (Zn, Cu, Cr, and Co)

The vertical profiles of trace metals in both cores show three zones, supporting the results of sedimentary profiles but with variations in depth. In Core KH (Figure 6), the bottom portion (76–56 cm) shows nearly steady low trends, followed by a middle zone (56–18 cm) of increasing upward but very erratic trends and an uppermost zone (18–0 cm) marked by the enrichment of all the trace metals. In Core KM (Figure 7), different metals show different patterns within these three portions, probably reflecting different postdepositional behaviours. The profiles of Zn and Cu are similar to a large extent, with an increasing upward trend with some ups and downs in the bottom portion (70–56 cm), followed by a middle portion (56–30 cm) of gradual upward increase and a decreasing trend in the uppermost (30–0 cm) portion. Chromium shows a decreasing trend in the bottom portion, followed by an increasing trend in the second portion and finally an erratic distribution in the upper portion. Cobalt values show an increasing trend in the bottom portion, as do Zn and Cu, and then an erratic trend in the middle portion and a gradually increasing upward trend in the top portion.

In order to assess elemental association, correlation tests were carried out for the data set of each core (Table 3). Analysis of the correlation coefficients among the different chemical components for Core KH shows a significant correlation

of Al with Fe (0.78), Mn (0.86), Cu (0.65), Cr (0.63), K (0.75), and Mg (0.63), while in Core KM, Al shows a significant correlation with Fe (0.90), Mn (0.81), Zn (0.66), Cu (0.75), Co (0.76), K (0.87), except with Mg (0.48). This strong correlation with Al indicates that metals are dominantly associated with clay minerals, probably as lattice-bound components (Rosales-Hoz, Cundy, and Bahena-Manjarrez, 2003).

Further, in Core KH, Fe and Mn show a significant correlation with Cu (0.67 and 0.71, respectively) and Cr (0.65 and 0.72, respectively), suggesting that Cu and Cr are associated with Fe and Mn oxyhydroxides. In Core KM, Fe shows a significant correlation with Co (0.71) and Cu (0.80) while Mn shows a significant correlation with Co (0.79) only. The similarity in the profiles of Cu and Zn ($R = 0.71$) with depth in Core KM and their significant association with Fe only suggests that the distribution of Cu and Zn may be more strongly controlled by Fe cycling than Mn cycling. Allen, Rae, and Zanin (1990) identified a similar pattern for Cu, Pb, and Zn in sediments from the Severn Estuary. On the other hand, Co shows a better association with Mn than Fe in Core KM and in the top oxic layer in Core KH, reflecting that Co is more cycled along with Mn oxides at redox boundaries (Zwolsman, Berger, and Van Eck, 1993). The exclusive role played by Mn oxides in the cycling of Ni and Co has been reported earlier by Klinkhammer (1980) and Shaw, Gieskes, and Jalinke (1990).

Evidence of digenetic modifications can be seen below the oxic-suboxic interface of the cores due to the dissolution of Fe and Mn oxyhydroxides. In Core KM, the peaks of Zn and Cu at depths of 52 cm and 56 cm, and the peaks at 66 cm and 70 cm for Zn, Cu, and Cr coincide with Fe peaks; this probably indicates the coprecipitation of these elements. The trace metal profiles in Core KH also seem to be altered by postdepositional processes. For instance, peaks of Cu and Co at 8 cm in the upper portion coincide with Fe and Mn enrichment. This evidence of heavy metal coprecipitation with Fe and Mn oxides may be related to porewater movement during reduction and re-adsorption in the oxic zone (Finney and Huy, 1989). Hence cycling of Fe and Mn may partly control the vertical profile of trace metals in these sediments.

Organic carbon and clay contents are the major controlling factors, which influence the binding of heavy metals (De Groot, Salomons, and Allersma, 1976; Fletcher, Bubbs, and Lester, 1994; Williams, Bubb, and Lester, 1994). The association of heavy metals, including Fe and Mn, with finer fractions in both the cores can be demonstrated through correlation of metal concentrations with sediment components (Table 3). In Core KH, mud (silt and clay) shows a significant positive correlation of 0.88 with Fe, 0.90 with Mn, 0.66 with Cu, and 0.74 with Cr, whereas sand shows a strong negative correlation with the same elements (-0.89 Fe, -0.92 Mn, -0.69 Cu, and -0.74 Cr). In Core KM, mud shows a significant positive correlation of 0.88 with Fe (0.78 silt, 0.79 clay), 0.90 with Mn (0.77 silt, 0.83 clay), 0.67 with Zn (0.68 silt, 0.52 clay), 0.71 with Cu (0.67 silt, 0.60 clay), and 0.80 with Co (0.70 silt, 0.74 clay), whereas sand shows a strong negative correlation with the same elements (-0.88 Fe, -0.90 Mn, -0.67 Zn, -0.71 Cu, and -0.80 Co).

Similarly, the influence of organic carbon in heavy metal distribution can be seen in Core KH, even though overall organic carbon content is low. However, the degree of correlation does not support the controls on heavy metal distribution in Core KM. During initial deposition, trace metals may become associated with organic matter (Salomons and Forstner, 1984). Metals may be redistributed by early aerobic degradation of organic matter, resulting in a gradual decrease in metal concentration with depth (Allen, Rae, and Zanin, 1990; Valette-Silver, 1993). In Core KH, values of organic carbon show a more or less decreasing trend with depth, and the concentrations of Fe, Mn, Cu, and Cr show a characteristic decrease with depth, which suggests that metals have been significantly redistributed by the degradation of organic carbon. The redistribution of metals by the degradation of organic carbon is also supported by the significant correlation of organic carbon with Fe (0.61), Mn (0.72), Cu (0.62), and Cr (0.73). This can probably be attributed to the percolation of oxygen-rich porewater in this sandy mudflat during high tides, which allows the degradation of organic carbon. Selvaraj *et al.* (2003) have reported the clear early diagenetic signal due to percolation of oxygen-rich porewater, which allows the oxidation-reduction changes in the sand-dominated intertidal region. However, the phenomenon cannot be applied to Core KM, as there is little evidence to suggest the association of metals with organic carbon because correlation values are poor (Fe, 0.23; Mn, 0.36; Zn, 0.03; Cu, 0.01; Cr, -0.09; Co, 0.21). This is probably due to oxygen-depleted, more–protected, and muddy sediment in which there is less chance of aeration and hence no degradation. Further, in this condition, the distribution of trace metals is probably controlled by the mud as well as by redox-sensitive Fe and Mn oxides. Similar phenomena have been reported earlier by Ayyamperumal *et al.* (2006) and Spencer, Cundy, and Croudace (2003).

Intercore Variations

Geochemical data from surface sediments and cores frequently show variations due to one or more factors: mineral variations (change in clay, sand, carbonate, or particulate organic matter inputs), redox-controlled element migration, and pollution (Cearreta *et al.,* 2000). A difference in sediment components, organic carbon, and metal distributions are observed between the two cores, which could be because of differences in source, sedimentary processes, and depositing site. These variations can be clearly seen through plotted isocon diagrams (Figure 8). An isocon diagram is a simple yet effective way of showing how concentrations vary between the different cores (Cundy *et al.,* 1997; Grant, 1986). It allows a simple visual comparison of the average composition of the sediments at each site (Rosales-Hoz, Cundy, and Bahena-Manjarrez, 2003). The isocon diagrams showed that there was little difference in the major elements Al and K and heavy metals Zn and Cu, which are plotted on or near the isocon line (indicating little variation). The differences are most apparent with higher concentrations of Ca, Co, and sand in Core KH, while Mg, Fe, Mn, Cr, clay, and OC are higher in Core KM. This higher amount of Fe, Mn, and OC in Core KM is clearly due to their association with finer frac-

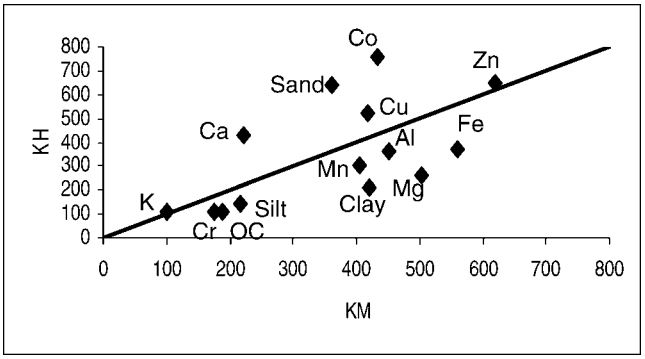

Figure 8. Isocon diagram. Individual points represent the average value of sediment components and elements in each core. To ensure all elements plot on the same scale, major elements by percentage (Al, K, Mg, Fe, and OC) are multiplied by 100; Ca, Cr, and Mn (in ppm) by 1; and Zn, Cu, Co, sand, silt, and clay by 10.

tion of sediments (clay and silt), which is also high in this core. In intertidal flats where sulfate reduction is dominant, metal ions are more likely to be precipitated as insoluble through sediment if the extent of water percolation through that sediment is limited (Warren, 1981). This process may partially account for a higher metal concentration as seen in Core KM, which is more protected and less porous. The marine influence is more visible in Core KH by higher concentrations of Ca with an increase in grain size. Some metals such as Zn and Cr form strong complexes with chloride ligands, and therefore changes in salinity may have profound effects on their solubility (Forstner and Salomons, 1980). In fact, Cr concentration in Core KH is comparatively less than in Core KM, where the change in salinity is more pronounced. Further, there is a higher concentration of Mn in core KM, with enrichment in the upper portion. Manganese oxides are reduced in anoxic sediments to more soluble oxide forms like Mn^{2+}, which can enter the interstitial waters of the sediment (Beeftink and Rozema, 1988). The anoxic conditions present in the tidal flats may facilitate the reduction of Mn oxides in both cores; however, a higher amount of percolation facilitates removal of a substantial amount of Mn in sandy Core KH, where the tidal actions and change in salinity is more pronounced.

CONCLUSIONS

Grain size analysis indicates a highly variable depositional regime with fining up of the core. The analysis reveals the possibility of three episodes of deposition in both cores. Organic carbon is comparatively high in muddy Core KM, which was collected from a more sheltered creek with a narrow mouth interior to the estuarine environment; it is comparatively low in sandy Core KH, which was collected from a creek with a wide mouth nearer to the sea. However, the distribution of OC with depth in Core KH was controlled by the proportion of finer fraction, which was not the case in muddy Core KM.

Geochemical data show an upper zone of marked enrichment of all trace metals, including Fe and Mn, in both cores. The distribution of Fe, Mn, Cu, and Cr in Core KH are partly controlled by clay fraction and OC, while mud, Fe, and Mn controlled distribution of Zn, Cu, and Co in Core KM.

The vertical profiles indicate that Mn, and to some extent Fe, in both cores have been remobilized and that these diagenetic processes have modified the vertical distributions of Cu, Zn, Cr, and Co. In Core KH, there is evidence of redistribution of metals by early aerobic degradation of organic matter, in addition to the role played by clay fraction and Fe and Mn oxyhydroxides, resulting in a gradual decrease in metal concentration with depth. The distribution of trace metals in Core KM is probably solely controlled by the mud and by redox-sensitive Fe and Mn oxides. Further, the geomorphological setup of the two creeks and therefore the tidal circulation would also have played an important role in the vertical distribution of sediments and their associated metals.

ACKNOWLEDGMENTS

The authors would like to thank Dr. Rafael Fernandes, faculty member of the Department of English, Goa University, for his constructive suggestions, which have helped in improving the English language of the paper.

LITERATURE CITED

Allen, J.R.L. and Duffy, M.J., 1998. Temporal and spatial depositional patterns in the Severn Estuary, southwestern Britain: intertidal studies at spring—neap and seasonal scales, 1991–1993. *Marine Geology,* 146(1–4), 147–171.

Allen, J.R.L.; Rae, J.E., and Zanin, P.E., 1990. Metal speciation (Cu, Zn, Pb) and organic matter in an oxic salt marsh, Severn Estuary, Southwest Britain. *Marine Pollution Bulletin,* 21, 574–580.

Ayyamperumal, T.; Jonathan, M.P.; Srinivasalu, S.; Armstrong-Altrin, J.S., and Ram-Mohan, V., 2006. Assessment of acid leachable trace metals in sediment cores from River Uppanar, Cuddalore, Southeast coast of India. *Environmental Pollution,* 143, 34–45.

Bangnold, R.A., 1968. Deposition in process of hydraulic transport. *Sedimentology,* 10, 45–56.

Beeftink, W.G. and Rozema, J., 1988. The nature and functioning of saltmarshes. *In:* Salomans, W. and Forstner, U. (eds.), *Pollution of the North Sea, An Assessment.* Berlin: Springer, pp. 59–87.

Billon, G.; Ouddane, B., and Boughriet, A., 2002. Chemical speciation of sulfur compounds in the surface sediments from the three bays (Freshnaye, Seine and Authie) in northern France, and identification of some factors controlling their generation. *Talanta,* 53, 971–981.

Biscaye, P.E., 1965. Mineralogy and sedimentation of recent deep-sea clay in the Atlantic Ocean and adjacent seas and oceans. *Geological Society of America Bulletin,* 76, 803–832.

Borrego, J.; Lopez-Gonzalez, N., and Carro, B., 2004. Geochemical signature as markers in Holocene sediments of the Tinto River estuary (Southwestern Spain). *Estuaries, Coastal and Shelf Science,* 61, 631–641.

Cearreta, A.; Irabien, M.J.; Leorri, E.; Yusta, I.; Croudace, I.W., and Cundy, A.B., 2000. Recent anthropogenic impacts on the Bilbao estuary, northern Spain: geochemical and microfaunal evidence. *Estuarine, Coastal and Shelf Science,* 50, 571–592.

Chamley, H., 1989. *Clay Sedimentology.* Berlin: Springer, 623p.

Cundy, A.B. and Croudace, I.W., 1995. Sedimentary and geochemical variations in a salt marsh/mudflat environment from the mesotidal Hamble estuary, southern England. *Marine Chemistry,* 51, 115–132.

Cundy, A.B.; Croudace, I.W.; Thomson, J., and Lewis, J.T., 1997. Reliability of salt marshes as 'geochemical recorders' of pollution

input: a case study from contrasting estuaries in southern England. *Environmental Science and Technology,* 31, 1093–1101.
Davies-Colley, R.J.; Nelson, P.O., and Williamson, K.H., 1984. Copper and cadmium uptake by estuarine sedimentary phases. *Environmental Science and Technology,* 18, 491–499.
De Groot, A.J.; Salomons, W., and Allersma, E., 1976. Processes affecting heavy metals in estuarine sediments. *In:* Burton, J.D. and Liss, P.S. (eds.), *Estuarine Chemistry.* London: Academic Press, pp. 131–157.
Finney, B.P. and Huy, C., 1989. History of metal pollution in the Southern California Bight: an update. *Environmental Science and Technology,* 23, 294–303.
Flemming, B.W., 2000. A revised textural classification of gravel-free muddy sediments on the basis of ternary diagrams. *Continental Shelf Research,* 20, 1125–1137.
Fletcher, C.A.; Bubb, J.M., and Lester, J.N., 1994. Magnitude and distribution of anthropogenic contaminants in salt marsh sediments of the Essex coast, UK. I. Topographical, physical and chemical characteristics. *Science of the Total Environment,* 155, 31–45.
Folk, R.L., 1968. *Petrology of Sedimentary Rocks.* Austin, Texas: Hemphills, 177 pp.
Forstner, U. and Salomons, W., 1980. Trace metal analysis in polluted sediments: Part I. Assessment of sources and intensities. *Environmental Technology Letters,* 1, 494–505.
Gallagher, K.A.; Wheeler, A.J., and Oxford, J.D., 1996. An assessment of the heavy metal pollution of two tidal marshes on the North West Coast of Ireland. *Biology and Environment: Proceedings of the Royal Irish Academy,* 96B(3), 177–188.
Gaudette, H.E.; Flight, W.R.; Toner, L., and Folger, D.W., 1974. An inexpensive titration method for the determination of organic carbon in recent sediments. *Journal of Sedimentary Petrology,* 44, 249–253.
Grant, J.A., 1986. The isocon diagram—a simple solution to Gresen's equation for metasomatic alteration. *Economic Geology,* 81, 1976–1982.
Grant, S.H. and Middleton, R., 1990. An assessment of metal contamination of sediments in the Humber Estuary, U. K. *Estuarine, Coastal and Shelf Science,* 31, 71–85.
Klinkhammer, G.P., 1980. Early diagenesis in sediments from the eastern equatorial Pacific, II. Pore water metal results. *Earth and Planetary Science Letters,* 49, 81–101.
Lesueur, P.; Lesourd, S.; Lefebvre, D.; Granaud, S., and Brun-Cottan, J., 2003. Holocene and modern sediments in the Seine estuary (France): a synthesis. *Journal of Quaternary Science,* 18(1), 3–16.
Louma, S.N. and Bryan, G.W., 1982. A statistical study of environmental factors controlling concentrations of heavy metals in the burrowing bivalve Scrobicularia plana and polychaete Nereis diversicolor. *Estuarine, Coastal and Shelf Science,* 15, 95–108.
McCaffrey, R.J. and Thomson, J., 1980. A record of the accumulation of sediments and trace metals in a Connecticut, USA, salt marsh. *Advanced Geophysics,* 22, 165–236.
Nayak, G.N., 1993. *Beaches of Karwar: Morphology, Texture and Mineralogy.* Panaji, India: P. Bhinde, 194p.
Nayak, G.N., 1996. Grain size parameters as indicator of sediment movement around river mouth, near Karwar, west coast of India. *Indian Journal of Marine Science,* 25(4), 346–348.
O'Brien, D.J.; Whitehouse, R.J.S., and Cramp, A., 2000. The cyclic development of a macrotidal mudflat on varying timescales. *Continental Shelf Research,* 20(12–13), 1593–1619.
Patersion, D.M.; Crawford, R.M., and Little, C., 1990. Subaerial exposure and changes in the stability of intertidal estuarine sediments. *Estuarine, Coastal and Shelf Science,* 30, 541–556.
Rao, V.P. and Rao, B.R., 1995. Provenance and distribution of clay minerals in the sediments of the western continental shelf and slope of India. *Continental Shelf Research,* 15, 1757–1771.
Rosales-Hoz, L.; Cundy, A.B., and Bahena-Manjarrez, J.L., 2003. Heavy metals in sediment cores from a tropical estuary affected by anthropogenic discharges: Coatzacoalcos estuary, Mexico. *Estuarine, Coastal and Shelf Science,* 58, 117–126.
Rule, J.H. and Alden, R.W., 1996. Interactions of Cd and Cu in aerobic estuarine sediments: II. Bioavailability, body burdens, and respiration effects as related to geochemical partitioning. *Environmental Toxicology and Chemistry,* 15(4), 466–471.
Salomons, W. and Forstner, U., 1984. *Metals in the Hydrocycle.* Berlin: Springer, 349p.
Selvaraj, K.; Ram Mohan, V.; Srinivasalu, S.; Jonathan, M.P., and Siddartha, R., 2003. Distribution of nondetrital trace metals in sediment cores from Ennore Creek, Southwest Coast of India. *Journal of the Geological Society of India,* 62, 191–204.
Shaw, T.J.; Gieskes, J.M., and Jalinke, R.A., 1990. Early diagenesis in differing depositional environments: the response of transitional metals in pore water. *Geochimica et Cosmochimica Acta,* 54, 1233–1246.
Shea, D., 1988. Developing national sediment quality criteria. *Environmental Science and Technology,* 22, 1256–1261.
Singer, A., 1984. The paleoclimate interpretation of clay minerals in the sediments—a review. *Earth Science Reviews,* 21, 251–293.
Spencer, K.L.; Cundy, A.B., and Croudace, I.W., 2003. Heavy metal distribution and early diagenesis in salt marsh sediments from the Medway Estuary, Kent, UK. *Estuarine, Coastal and Shelf Science,* 57, 43–54.
Thomson, J.; Dyer, F.M., and Croudace, I.W., 2002. Records of radionuclide deposition in two salt marshes in the United Kingdom with contrasting redox and accumulation conditions. *Geochimica et Cosmochimica Acta,* 66, 1011–1023.
Valette-Silver, N.J., 1993. The use of sediment cores to reconstruct historical trends in contamination of estuarine and coastal sediment. *Estuaries,* 16, 577–588.
Veer, M.P.; Shanmukhappa, H., and Bhat, U.G., 1992. Copper, chromium and manganese in water and sediment of Kali estuary, Karwar. *Fishery Technology. Society of Fisheries Technologists (India),* 29(1), 27–29.
Vilas, F.; Arche, A.; Ferrero, M., and Isla, F., 1999. Subantarctic macrotidal flats, cheniers and beaches in San Sebastian Bay, Tieera del Fuego. *Marine Geology,* 160, 301–326.
Warren, L.J., 1981. Contamination of sediments by lead, zinc and cadmium: a review. *Environmental Pollution,* B2, 401–436.
Williams, T.P.; Bubb, J.M., and Lester J.N., 1994. Metal accumulation within salt marsh environments: a review. *Marine Pollution Bulletin,* 28, 277–290.
Yallop, K.M.; De Winter, B.; Paterson, D.M., and Stal, L.J., 1994. Comparative structure, primary production and biogenic stabilization on cohesive and non-cohesive marine sediments inhabited by micro-phytobenthos. *Estuarine, Coastal and Shelf Science,* 39, 565–582.
Zwolsman, J.J.G.; Berger, G.W., and Van Eck, G.T.M., 1993. Sediment accumulation rates, historical input, post-depositional mobility and retention of major elements and trace elements in salt marsh sediments of the Scheldt estuary, SW Netherlands. *Marine Chemistry,* 44, 73–94.